ISSN 1070-4272, Russian Journal of Applied Chemistry, 2023, Vol. 96, No. 3. pp. 297–309. © Pleiades Publishing, Ltd., 2023.
Russian Text © The Author(s), 2023, published in Zhurnal Prikladnoi Khimii, 2023, Vol. 96, No. 3, pp. 269–281.

INORGANIC SYNTHESIS AND INDUSTRIAL INORGANIC CHEMISTRY

Impact of Precursor Granulometry on the Synthesis of Calcium-Aluminate Phases

M. A. Trubitsyn[a,*], L. V. Furda[a], M. N. Yapryntsev[a], N. A. Volovicheva[a], and M. O. Mikhailyukova[a]

[a] *Belgorod State National Research University, Belgorod, 308015 Russia*
**e-mail: troubitsin@bsu.edu.ru*

Received May 17, 2023; revised September 27, 2023; accepted October 19, 2023

Abstract—Calcium aluminate phases were synthesized in the range 950–1450°C from available raw materials: carbonate rock and metallurgical alumina, predominantly in the γ form with different grain sizes. The calculations of the amount of raw materials were based on the requirement to ensure the chemical composition of the product: Al_2O_3 71–72 and CaO 27–28 wt %. The designed phase composition of the samples is 65 wt % $CaAl_2O_4$ and 35 wt % $CaAl_4O_7$. When alumina with a grain size of 90 μm and a spherulitic microstructure is introduced into the reaction, the formation of the $CaAl_2O_4$ and $CaAl_4O_7$ phases mainly occurs in the range of 1250–1350°C, and phase equilibrium is established at 1450°C. Reducing the size of γ-alumina grains to 10 μm and destroying their spherulitic microstructure shifts the formation of calcium aluminates to the temperature range below 1250°C, and also significantly increases the rate of synthesis of target products.

Keywords: calcium aluminate phases, solid phase reaction, grain size, microstructure

DOI: 10.1134/S1070427223030059

The $CaO–A1_2O_3$ phase diagram is used to determine the types and equilibrium composition of calcium aluminate phases depending on the molar ratio of precursors and process parameters. According to literature data [1–4], in the $CaO–A1_2O_3$ system, depending on the CaO/Al_2O_3 molar ratio, the following phases can exist: $Ca_3Al_2O_6$, $Ca_{12}Al_{14}O_{33}$, $CaAl_2O_4$, $CaAl_4O_7$, and $CaAl_{12}O_{19}$. $CaAl_2O_4$ and $CaAl_4O_7$, which are the main phases of calcium aluminate cements, are of greatest practical importance. These materials are widely used in the refractory, metallurgical, and construction industries [5]. In recent years, calcium aluminates were included in optical [6], structural ceramics [7], and biomaterials [8].

There is a sufficient number of works in the literature devoted to the synthesis and study of the mechanisms of formation of monophasic products, primarily $CaAl_2O_4$ [9–13]. For example, in [9], the kinetics of the synthesis reaction of $CaAl_2O_4$ from CaO and α-Al_2O_3 was studied in the range of 1150–1400°C. The phases $Ca_3Al_2O_6$ and $Ca_{12}Al_{14}O_{33}$ were found to be intermediate in the formation of $CaAl_2O_4$. The kinetics of $CaAl_2O_4$ formation from these oxides is well described by the Ginstling–Brownstein diffusion model.

The way of producing high-purity $CaAl_2O_4$ from pre-ground mixtures of $CaCO_3$ and α-Al_2O_3 or amorphous $Al(OH)_3$ is known [10]. The formation of intermediate phases $Ca_{12}Al_{14}O_{33}$ and $CaAl_4O_7$ from a powder mixture of α-Al_2O_3 and $CaCO_3$ was observed at 900 and 1100°C, respectively, and the presence of these phases was recorded at 900°C when using $Al(OH)_3$ and $CaCO_3$. The final formation of $CaAl_2O_4$ was detected at 1300°C. It is noted that this temperature is lower than that required for the formation of $CaAl_2O_4$ in the traditional solid-phase reaction process.

Studies of the processes of joint synthesis of the $CaAl_2O_4$ and $CaAl_4O_7$ phases are scarce. According to work [14], in the low temperature region of 600–900°C, the formation of $Ca_{12}Al_{14}O_{33}$ occurs, followed by the production of $CaAl_2O_4$. Upon the temperature increases, the interaction of alumina with CaO accelerates, resulting in a significant increase in the amount of $CaAl_2O_4$ and a

Table 1. Chemical composition of raw materials, wt %

Material	Al_2O_3	SiO_2	Fe_2O_3	CaO	MgO	Na_2O	Loss on calcination
Alumina of G-00 grade	98.600	0.020	0.015	Traces	Traces	0.100	1.265
Carbonate rock of M-90 grade	0.100	0.100	0.080	55.200	Traces	Traces	44.520

Table 2. Textural characteristics of raw materials

Material	Granulometric composition[a]				Specific surface area (Brunauer–Emmett–Teller method), $m^2\ g^{-1}$
	D_{90}, μm	D_{50}, μm	D_{20}, μm	content of submicrometer fraction (≤1, μm), %	
Alumina of G-00 grade	149.60	89.02	60.53	–	61.38
Carbonate rock of M-90 grade	4.49	1.49	0.77	32.5	4.19

[a] D_{90}, D_{50}, D_{20} are particle size below which 90, 50, 20% of the material is contained, respectively.

decrease in the content of $Ca_{12}Al_{14}O_{33}$. At a temperature of 1000°C, when a significant part of CaO is bound in $CaAl_2O_4$, $CaAl_4O_7$ is synthesized due to the reaction between $CaAl_2O_4$ and Al_2O_3.

The formation of calcium aluminates in the temperature range 1200–1460°C using a reaction mixture of CaO and Al_2O_3 was studied in [15]. At 1250°C, the phases $Ca_3Al_2O_6$ and $Ca_{12}Al_{14}O_{33}$ were detected. It was found that $CaAl_2O_4$ is formed not through a direct reaction between CaO and Al_2O_3, but via the transformation of intermediate compounds. The formation of $CaAl_4O_7$ occurs due to the side reaction of the interaction of $CaAl_2O_4$ with Al_2O_3.

In [16], the phase formation process was studied using the example of a mixture of $CaCO_3$ and Al_2O_3 with initial grain sizes less than 10 and 1 μm, respectively. The synthesis of calcium aluminate phases was carried out at temperatures from 1300 to 1500°C with different isothermal keeping times. Upon a rise in the keeping time, a decrease in the amount of calcium-rich phase $Ca_{12}Al_{14}O_{33}$ was observed since it reacted with Al_2O_3 and to a lesser extent with $CaAl_4O_7$ to form $CaAl_2O_4$. The authors assert that the calcium-rich phases $Ca_{12}Al_{14}O_{33}$ and $Ca_3Al_2O_6$ do not act as intermediates, and $CaAl_4O_7$ is the result of a side reaction.

This work is aimed at studying the effect of the particle size distribution of available raw materials and thermal conditions on the processes of formation of the $CaAl_2O_4$ and $CaAl_4O_7$ phases.

EXPERIMENTAL

The calculation of the content of raw materials was based on the requirements of the technical specifications to ensure the chemical composition of the product: Al_2O_3 71–72 wt % and CaO 27–28 wt %. Designed equilibrium phase composition according to the CaO–$A1_2O_3$ phase diagram: 65 wt % $CaAl_2O_4$ and 35 wt % $CaAl_4O_7$.

The following raw materials were used in the work: natural fine carbonate rock of the Microcarb-90 (M-90) grade (JSC RUSLIME) and alumina of the G-00 grade (JSC RUSAL Achinsk Alumina Refinery). The chemical composition of alumina and carbonate rock according to the commercial product certificate and energy dispersive analysis, restectively, is presented in Table 1. The granulometric composition of raw materials was determined by laser diffraction (Table 2).

In terms of mineralogical composition, alumina of G-00 grade is represented predominantly by the crystalline phase γ-Al_2O_3, and carbonate rock of M-90 grade is represented by the mineral calcite $CaCO_3$.

To conduct the experiment, two raw mixtures were prepared. The first mixture included carbonate rock and alumina without preliminary grinding (composition index Al-0). The second raw mixture included carbonate rock and alumina, which was subjected to preliminary grinding in a laboratory ball mill ML-1 with a frequency controller (JSC NPTsK) for 2 h (composition index Al-2). Experimental samples for the synthesis of calcium

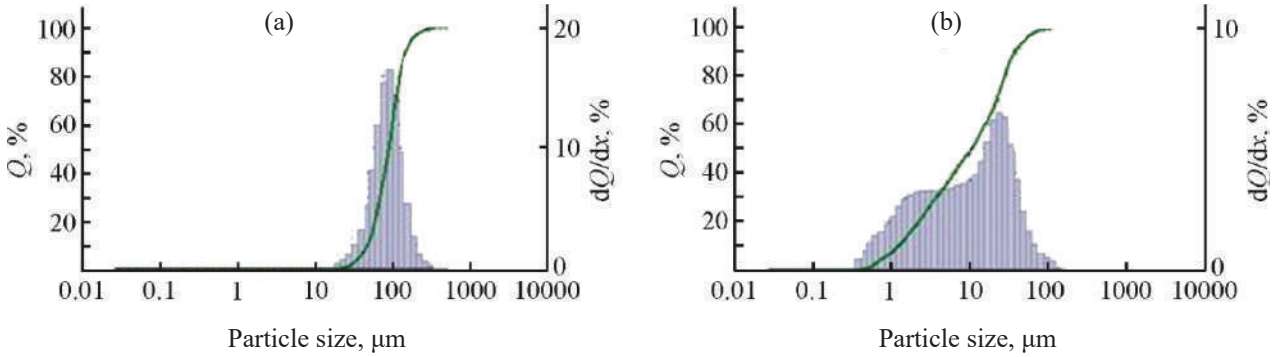

Fig. 1. Particle size distribution of alumina sample of G-00 grade: (a) initial raw material and (b) sample pre-ground for 2 h.

aluminate phases were prepared according to the method described in detail in [17].

Loss on calcining was measured by the gravimetric method in the temperature range of 300–1000°C. The study of the granulometric composition of materials was carried out on a Microtrac S3500 particle size analyzer (USA) using the laser diffraction method. Distilled water obtained by single distillation using an AE-15 medical electric water distiller (Livam PF LLC) was used as a dispersion medium in the study. The specific surface area of the powders was determined by low-temperature adsorption and thermal desorption of nitrogen using a TriStar II 3020 automated unit (Micromeritics).

Heat treatment of the samples was conducted in a high-temperature furnace LHT 02/17 (Nabertherm) according to the following regime: heating rate 250 deg h^{-1}, first isothermal keeping at a temperature of 900°C for 30 min, second isothermal keeping at specified maximum temperatures for 1 or 2 h. Thermal analysis was carried out using a combined thermal analyzer SDT Q 600 (TA Instruments) in an inert atmosphere at a heating rate of 10 deg/min^{-1} in the temperature range of 20–1400°C.

The phase composition of the materials was determined by X-ray phase analysis on a SmartLab diffractometer (Rigaku) using CuK_α radiation (λ = 1.54056 Å), Bragg–Brentano recording scheme, with a scanning speed of 2 deg min^{-1} in the 2θ angle range of 10°–70° s scanning step 0.02°. High-temperature X-ray phase analysis of the samples was conducted on the same device in the temperature range 25–1200°C with an isothermal keeping for 30 min. The PDF-2 database was used to identify peaks. Experimental diffraction patterns were processed using the PDXL program (Rigaku corporation) with refinement using the Rietveld method. The reference intensity ratio was calculated using corundum intensity as reference.

Morphological studies of materials were carried out with scanning electron microscopy (SEM) using a Nova NanoSEM 450 scanning electron microscope (FEI). Images were acquired using a backscattered electron detector in low vacuum mode, accelerating voltage 30 kV. The elemental composition of the samples was determined by energy dispersive analysis equipped with an attachment to the specified microscope.

RESULTS AND DISCUSSION

The nature of the distribution of particles in the G-00 alumina powder is monomodal with a maximum of ~100 μm (Fig. 1). The median particle size D_{50} is ~90 μm. The grain distribution of aluminous minerals after two hours of grinding is bimodal. The maximum of the first mode is not clearly expressed and corresponds to the range of 2–5 μm. The second mode is more intense and is recorded in the range of 20–30 μm. Median particle size D_{50} ~ 10 μm.

Alumina powder G-00 consists of spherulites 60–150 μm in size, which are closely packed agglomerates of prismatic particles (Fig. 2). At higher magnification, the slit-like pores formed due to the stack-shaped accretion of plate-shaped primary crystallites are clearly differentiated. After two hours of grinding the alumina, two types of particles are detected, differing in their morphological parameters. The first type includes fragments of spherulites, which are prismatic blocks of irregular shape, 10–50 μm in size, with a layered microstructure. The second group of particles

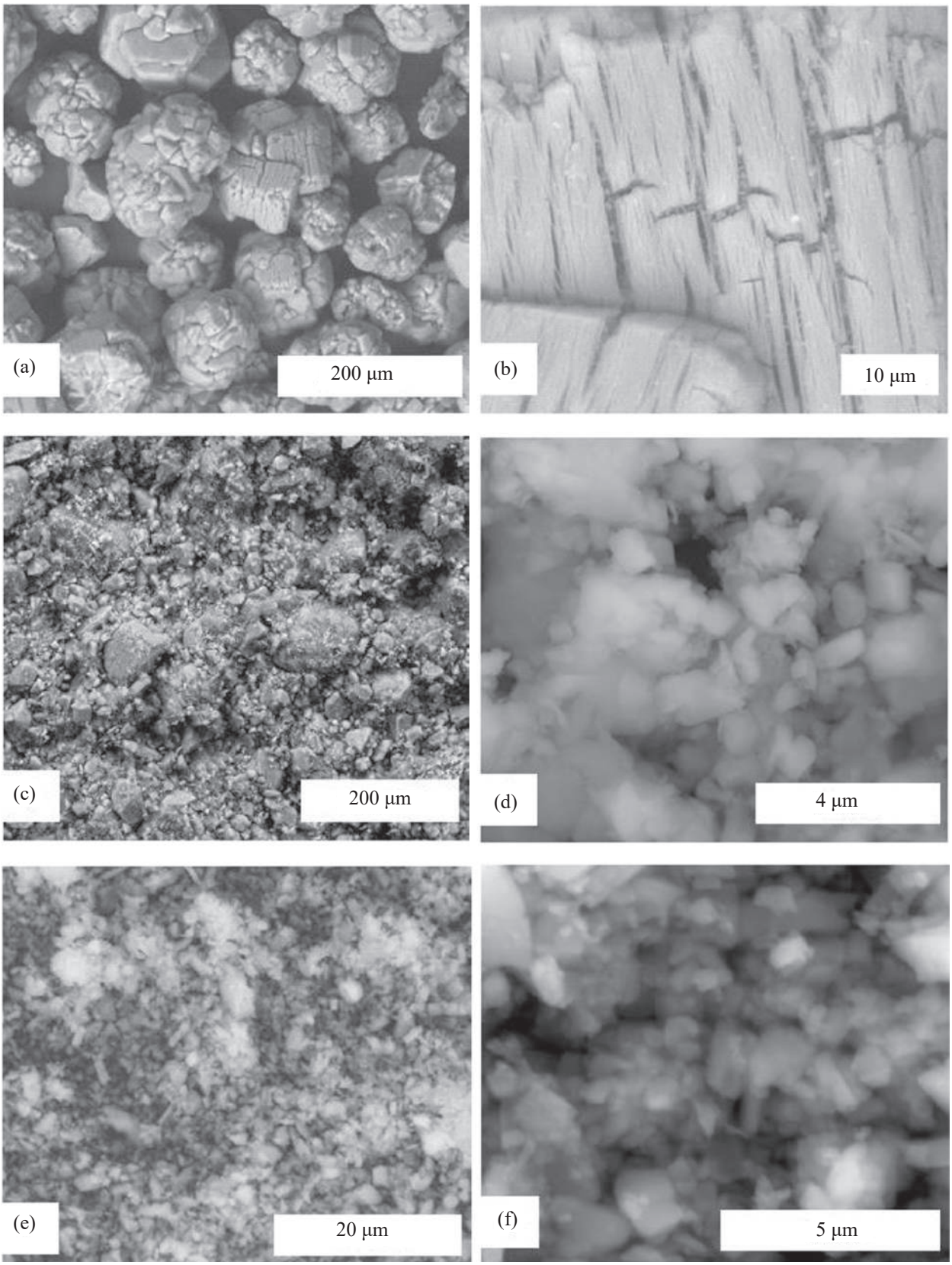

Fig. 2. Microphotographs of alumina powders of G-00 grade: (a, b) initial raw material, median grain size D_{50} ~ 90 μm and (c, d) a sample pre-ground for 2 h, median grain size D_{50} ~ 10 μm, as well as (e, f) carbonate rock of M-90 grade.

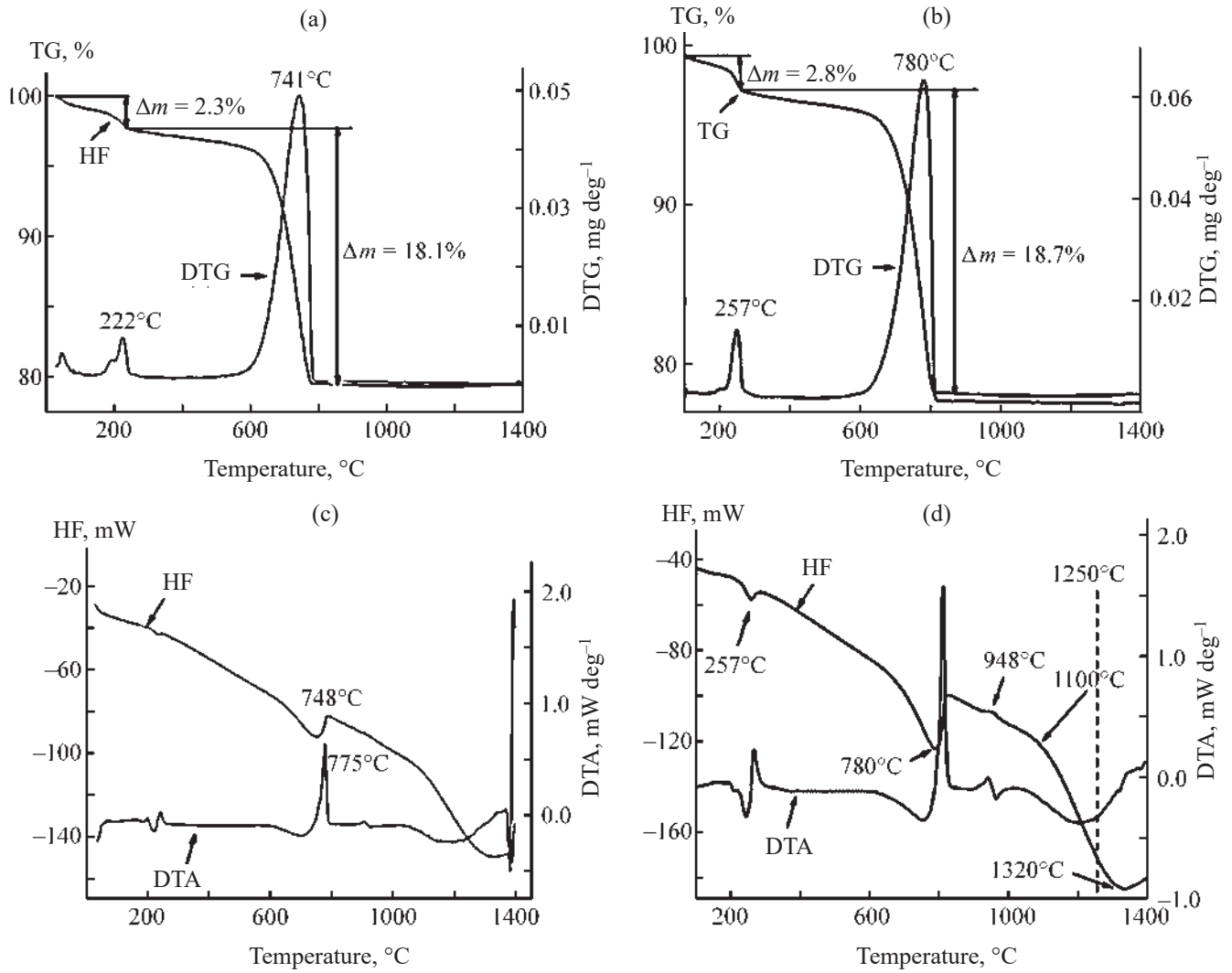

Fig. 3. Results of simultaneous thermal analysis of (a, c) samples of a mixture of carbonate rock of M-90 grade and initial alumina of G-00 grade with a median grain size of ~90 μm; (b, d) mixtures of carbonate rock of M-90 grade and ground alumina of G-00 grade with a median grain size of ~10 μm. TG, DTG, DTA are curves of thermogravimetric, differential thermogravimetric, differential thermal analysis, respectively; HF, heat flux.

is represented by acute-angled isometric plates 2–5 μm in size, which are evenly distributed between larger blocks. The microstructure of carbonate rock consists of plate-shaped finely dispersed grains with an average size of 1.5 μm, having an irregular acute-angled shape and demonstrating a tendency to aggregation.

Regardless of the method of preparing the mixtures, the thermal analysis curves are similar (Fig. 3). The differences lie in a slight shift in thermal effects at heating the Al-2 sample. This, in our opinion, is explained by a decrease in the size of alumina particles by approximately 9 times and a corresponding increase in their contact area with $CaCO_3$ particles. As a result, the dissociation of $CaCO_3$ and the release of water of crystallization are recorded at higher temperatures (by 40 and 30°C, respectively) than in the Al-0 sample.

The thermogravimetric (TG) and differential thermogravimetric (DTG) curves (Fig. 3) contain two extrema, which correspond to the maximum rate of change in the weight of the samples under study during the heating process. The positions of the extrema on the TG, DTG, heat flux (HF), and differential thermal analysis (DTA) curves coincide, which indicates the identity of the processes occurring in the system. In the

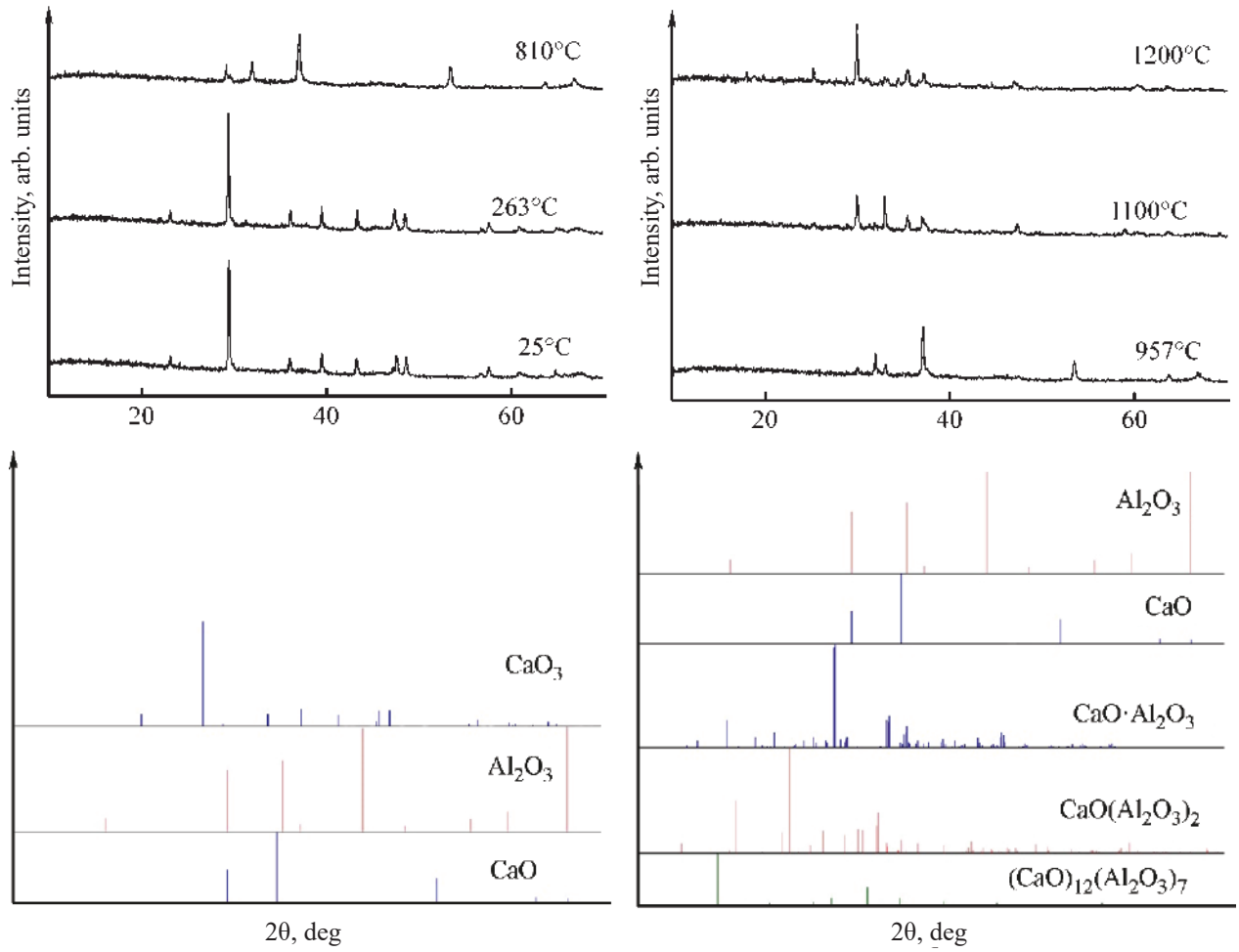

Fig. 4. Powder diffraction patterns of samples of a mixture carbonate rock of M-90 grade and ground alumina of G-00 grade (median grain size ~ 10 μm), heat-treated in the range of 25–1200°C, isothermal exposure for 30 min.

TG and HF curves up to a temperature of 200°C, there are an insignificant weight loss and an endothermic effect blurred by temperature. A more significant weight loss of the studied samples and the corresponding endothermic effect occur in the temperature range of 740–780°C. In our opinion, these effects are due to the removal of adsorption water and the decomposition of $CaCO_3$ with the formation of CaO.

According to [10], the exothermic effect at 948°C may be associated with the synthesis of $Ca_{12}Al_{14}O_{33}$. In the temperature range 1100–1400°C there is a wide endothermic effect associated with processes proceeding without changing the weight of the sample under study.

Preliminary studies of experimental mixtures showed that when the Al-0 sample is heated to 1000°C, only $CaCO_3$ dissociation occurs, while preliminary grinding of γ-alumina to D_{50} ~ 10 μm in this temperature range intensifies the processes of formation of calcium aluminates (Al-sample 2) (Fig. 4).

According to X-ray diffraction analysis at temperatures of 25 and 263°C, there are no changes in the phase composition. An increase in temperature to 810°C promotes the dissociation of $CaCO_3$ with the formation of CaO, which is accompanied by a decrease in the intensity of $CaCO_3$ reflexes and is confirmed by DTA data (Fig. 3). At a temperature of 957°C, reflexes corresponding to the phases $CaCO_3$, CaO, γ-Al_2O_3, and $Ca_{12}Al_{14}O_{33}$ were recorded. Further heating to 1100°C leads to the appearance of a significant amount of the $CaAl_2O_4$ phase (76%), while $Ca_{12}Al_{14}O_{33}$ and CaO are retained. At the same time, reflexes of γ-Al_2O_3 are no longer present. The latter is apparently due to the significant consumption of γ-Al_2O_3 for the synthesis of calcium aluminates and also to the X-ray amorphous

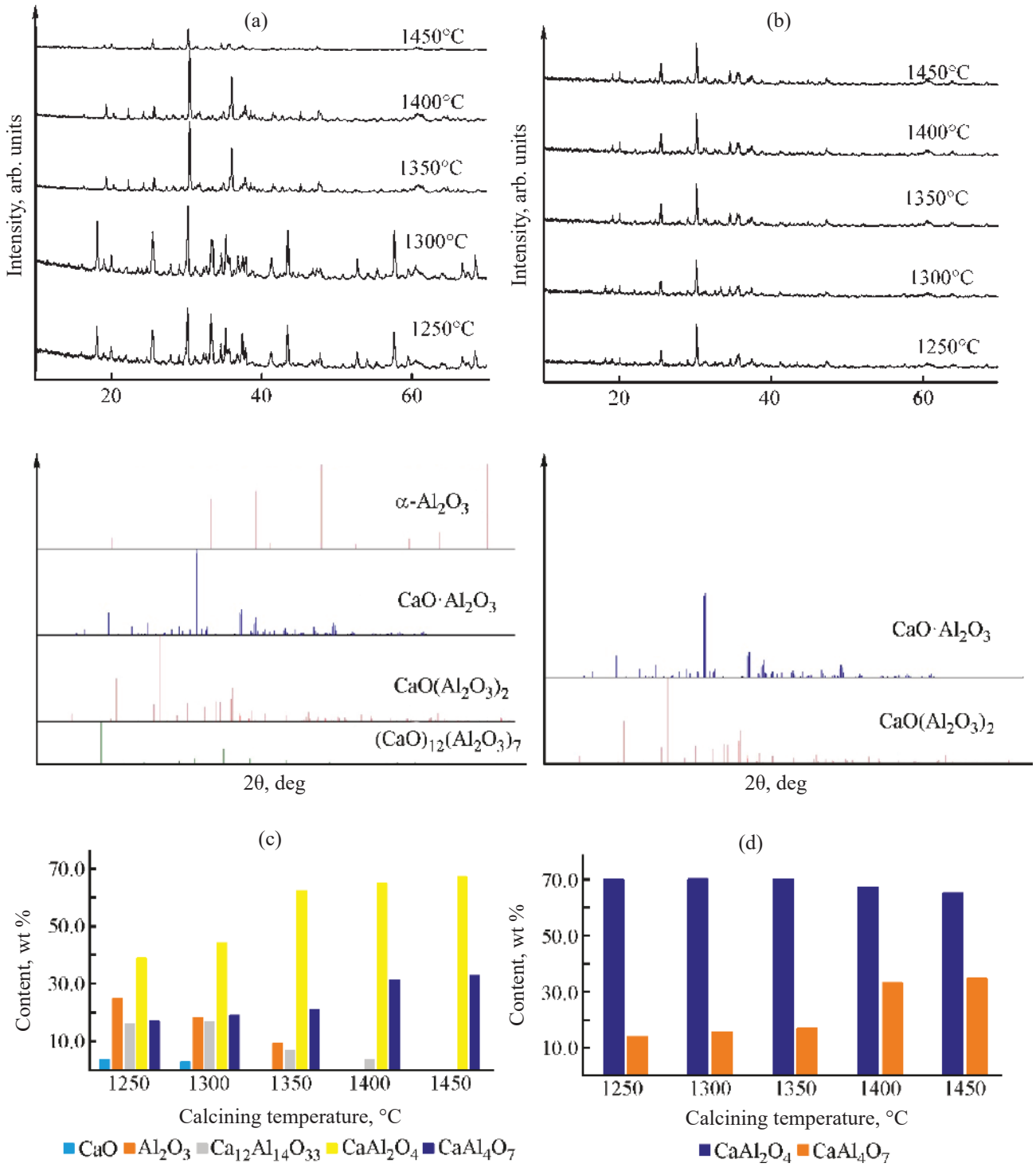

Fig. 5. Powder diffraction patterns and phase composition of experimental samples heat-treated at 1250–1450°C: mixtures of carbonate rock of M-90 grade and initial alumina of G-00 grade with a median grain size of ~90 μm, (a, c) isothermal exposure for 1 h, (e, g) isothermal keeping 2 h; (b, d) mixtures of carbonate rock of M-90 grade and ground alumina of G-00 grade with a median grain size of ~10 μm, (b, d) isothermal holding for 1 h, (f, h) isothermal holding for 2 h.

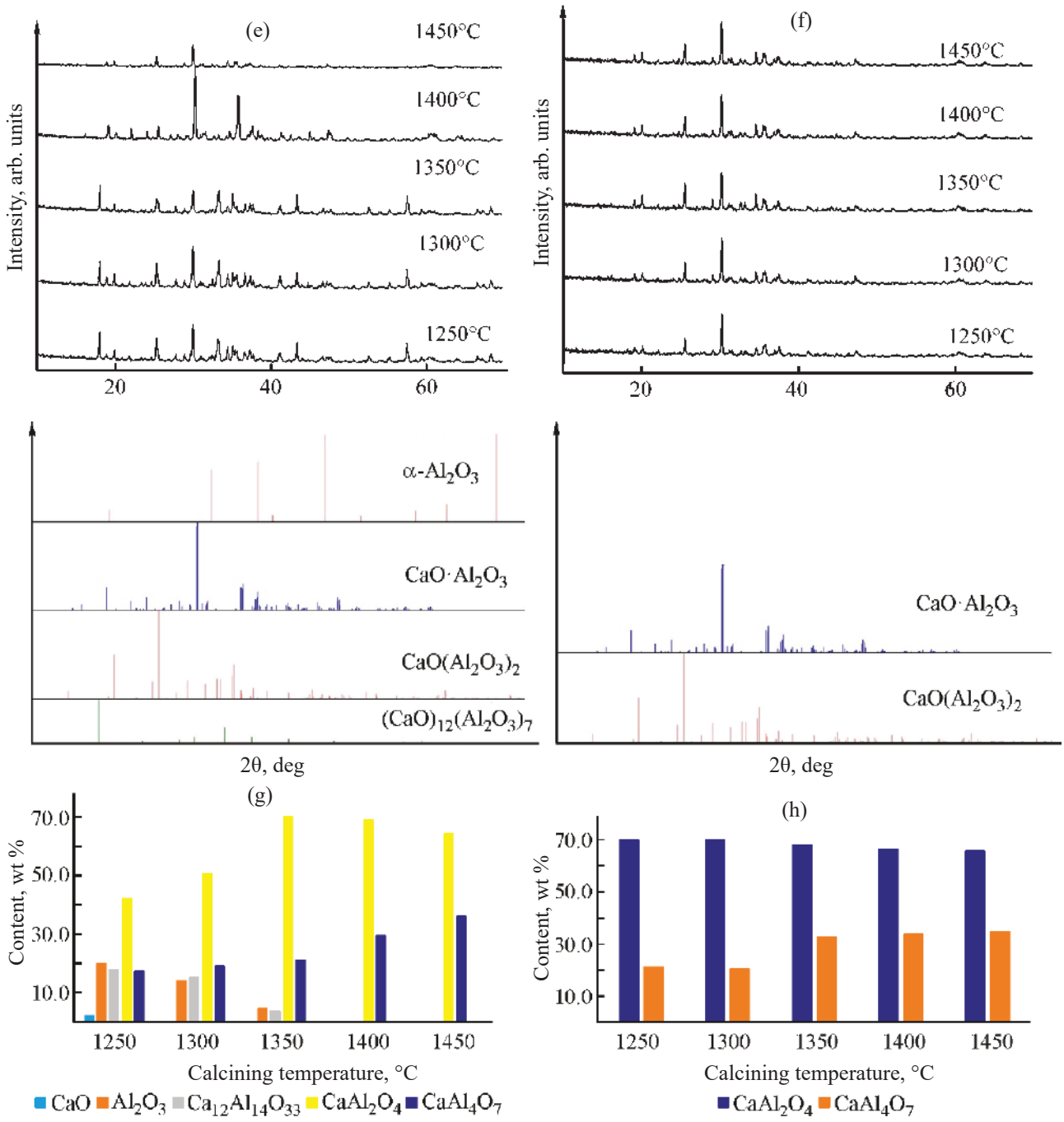

Fig. 5. (Contd.)

state of small amounts of unreacted precursor. Upon reaching a temperature of 1200°C, the presence of $CaAl_2O_4$, $CaAl_4O_7$, $Ca_{12}Al_{14}O_{33}$ is observed: 83.4, 10.3, and 6.3%, respectively.

To comparatively assess the effect of the particle size distribution and morphology of alumina on the phase formation processes, experimental samples of the Al-0 and Al-2 compositions were calcined at 1250, 1300, 1350, 1400, and 1450°C with isothermal keeping for 1 and 2 h (Fig. 5).

The main components of the Al-0 sample, kept for 1 h at a temperature of 1250°C (Figs. 5a, 5c), are the target phases $CaAl_2O_4$ (39.0 wt %) and $CaAl_4O_7$ (17.0 wt%). The α-Al_2O_3 and CaO phases are also

present: 24.5 and 3.5 wt %, respectively. The presence of $Ca_{12}Al_{14}O_{33}$ in an amount of 16.0 wt % indicates the beginning of the formation of phases enriched in calcium by the reaction between CaO and α-Al_2O_3. A further increase in the calcining temperature to 1300°C does not lead to a change in the content of $CaAl_2O_4$ and $CaAl_4O_7$ (44.3 and 18.7 wt %, respectively), and the content of CaO is 2.2 wt %. In this temperature range, a decrease in the intensity of α-Al_2O_3 reflexes (18.0 wt %) and a slight increase in the proportion of $Ca_{12}Al_{14}O_{33}$ (up to 16.8 wt %) are observed. Increasing the calcining temperature to 1350°C leads to the disappearance of CaO. The content of the intermediate phase $Ca_{12}Al_{14}O_{33}$ is 9.1 wt %, and those of $CaAl_2O_4$ and $CaAl_4O_7$ are 62.7 and 21.3 wt %, respectively.

In the calcining temperature range of 1250–1350°C, in samples containing pre-ground alumina to D_{50} ~10 μm (Al-2 composition), there are only the target phases $CaAl_2O_4$ and $CaAl_4O_7$, and their amount remains practically unchanged: 83.2–86.5 and 13.9–16.8 wt % respectively.

A further increase in the calcining temperature of Al-0 samples to 1400 and 1450°C leads to the complete disappearance of α-Al_2O_3 and the intermediate phase $Ca_{12}Al_{14}O_{33}$ (at 1450°C), the content of $CaAl_2O_4$ and $CaAl_4O_7$ is 65.0–67.2 and 31.5–32.8 wt %, respectively.

In samples of the Al-2 composition in this temperature range, a redistribution of the ratio of the target phases occurs, namely, the proportion of $CaAl_2O_4$ decreases to 65.0 wt %, and that of $CaAl_4O_7$ increases to 35.5 wt %.

In samples of composition Al-0 containing the initial alumina minerals (D_{50} ~ 90 μm), after calcining at 1250°C with isothermal keeping for 2 h, the amount of target phases $CaAl_2O_4$ and $CaAl_4O_7$, as well of phases $Ca_{12}Al_{14}O_{33}$, CaO, and α-Al_2O_3 has comparable values at similar temperature and keeping time for 1 h (Figs. 5g, 5c, respectively). In the case of heat treatment at 1300°C (isothermal keeping for 2 h), there is a tendency to reduce the amount of precursors (for CaO to 1.2 and for α-Al_2O_3 to 14.3 wt %) and the intermediate phase $Ca_{12}Al_{14}O_{33}$ to 14.5 wt %. This is probably due to the consumption of the above compounds to produce $CaAl_2O_4$ and $CaAl_4O_7$, the content of which increases to 50.8 and 19.2 wt %, respectively.

Under similar thermal conditions, samples of the Al-2 composition, including alumina pre-ground to D_{50} ~10 μm, contain only the $CaAl_2O_4$ (79.3–79.8 wt %) and $CaAl_4O_7$ (20.2–20.7 wt %) phases.

In the case of calcining Al-0 samples in the temperature range of 1350–1450°C with keeping for 2 h, the proportion of $CaAl_2O_4$ monotonically decreases (from 70.9 to 64.0 wt %), and the proportion of $CaAl_4O_7$ monotonically increases (from 21.4 to 36.0 wt %). Thus, after heat treatment at 1450°C, the content of the target phases becomes close to the design value (Figs. 5e, 5g).

At the same time, in Al-2 samples the design phase composition is practically achieved already at 1350°C. A further increase in temperature does not significantly affect the content of $CaAl_2O_4$ and $CaAl_4O_7$.

In the SEM image of the Al-0 sample (Fig. 6a), heat-treated at 1250°C, large spherulite particles (~100 μm) are observed, having a morphology identical to the grains of the original unground alumina (Fig. 2a). Closely packed α-Al_2O_3 globules are covered with finely dispersed CaO, which is a product of the decomposition of $CaCO_3$. In samples heat-treated at 1350°C, the formation of a layered microstructure of spherulites is clearly visible (Fig. 6c). The appearance of isthmuses between individual α-Al_2O_3 grains is detected as a consequence of the appearance of micromelts attributed to the accumulation in interphase locations of significant amounts of eutectoid phases enriched in calcium, primarily $Ca_{12}Al_{14}O_{33}$. The formation of micromelts intensifies the diffusion of Ca^{2+} to the core of high-alumina particles and the surface phase formation processes. A comprehensive analysis of the SEM image (Fig. 6c) and the results of X-ray diffraction analysis (Fig. 5e) suggest that the formation of the microstructure of calcium-aluminate phases of the core-shell type occurs due to the interaction of carbonate rock decomposition products (CaO) with surface aluminum-oxygen groups.

Heat treatment of samples at 1450°C leads to a significant increase in the amount of melt (Fig. 6e). As a result, the processes of diffusion and solid-phase interaction are intensified, which causes a significant rise in the synthesis rate of the $CaAl_2O_4$ and $CaAl_4O_7$ target phases.

The microstructure of Al-2 samples calcined at 1250°C is a collection of particles of different morphologies (Fig. 6b). Submicrometer round plates (less than 1 μm) surround larger isometric grains with a cellular structure (size ~10–20 μm). Regardless of size, all particles are connected through thin isthmuses caused by reaction sintering processes, which determines the formation of a unified communicating framework sys-

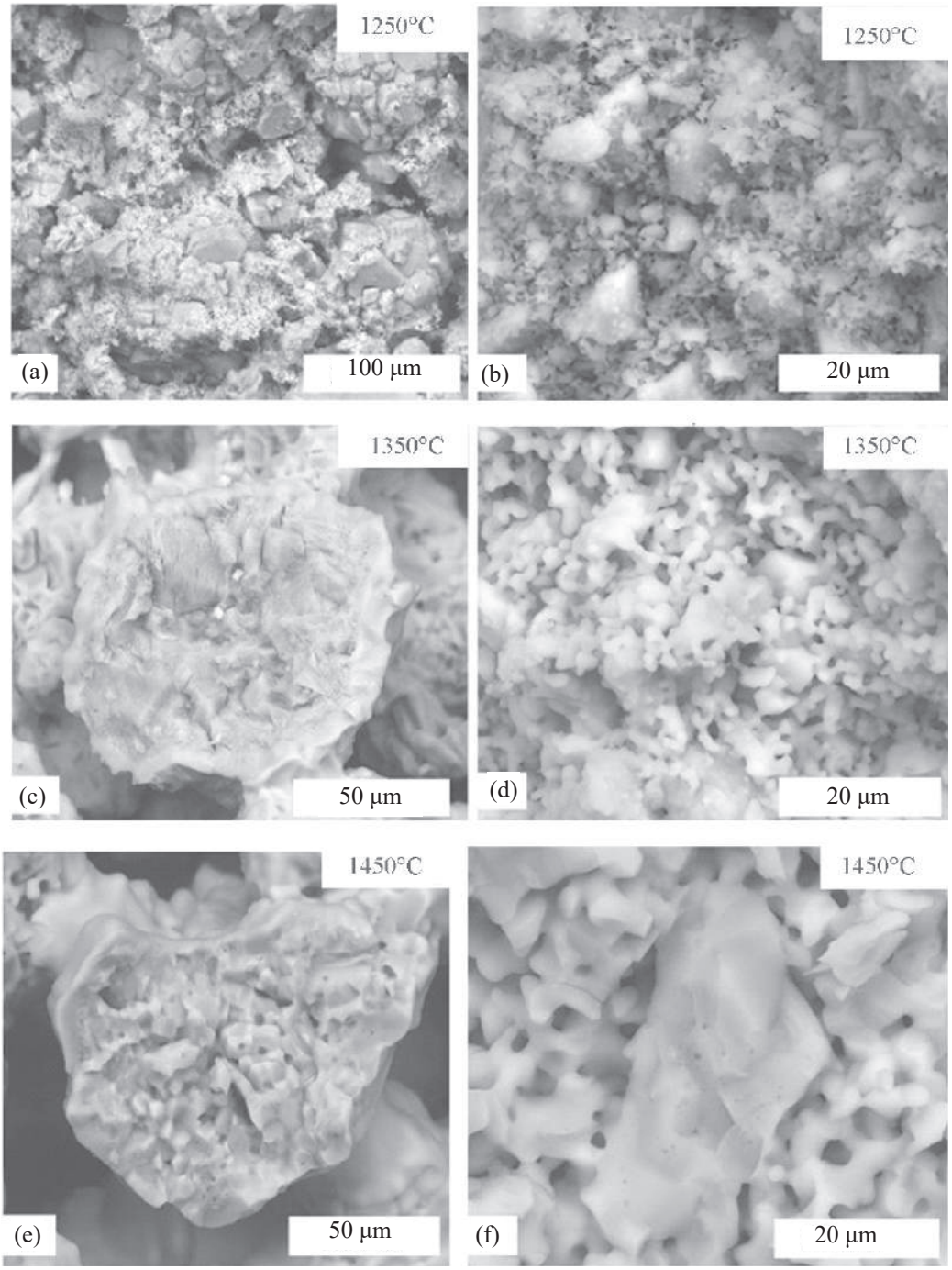

Fig. 6. Microphotographs of powders of (a, c, e) a mixture of carbonate rock of M-90 grade and initial alumina of G-00 grade with a median grain size of ~90 μm and (b, d, f) a mixture of carbonate rock of M-90 grade and ground alumina of G-00 grade with a median grain size of ~10 μm after heat treatment in the range of 1250–1450°C, isothermal keeping for 2 h.

tem. In our opinion, the appearance of such a framework system promotes low-temperature diffusion activity of Ca^{2+}. This explains the early formation of the $CaAl_2O_4$ and $CaAl_4O_7$ target phases at this temperature (Figs. 5f, 5h). In samples heat-treated at 1350 and 1450°C, there are an increase in the size of calcium aluminate crystals and further development of a continuous framework structure (Figs. 6d, 6f).

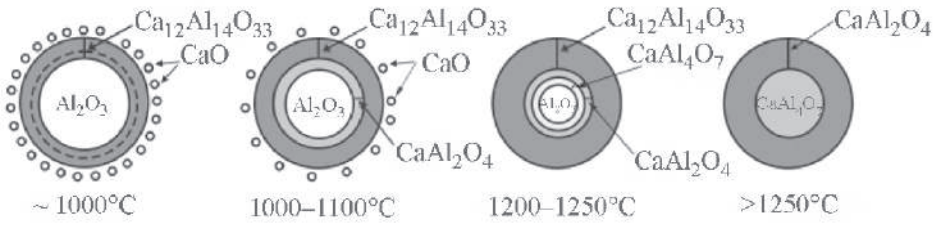

Fig. 7. Scheme of the sequence of formation of calcium-aluminate phases according to the core–shell type.

Taking into account the above, in our opinion, the results obtained can be interpreted as follows (Fig. 7).

In samples of composition Al-0, in places where spherulite grains γ-Al_2O_3 are localized, the primary act of solid-phase interaction of Ca^{2+} and AlO_4^{5-} ions at ~1000°C occurs directly on the interphase surface with the formation of $Ca_{12}Al_{14}O_{33}$ according to reaction (I). In the future, direct interaction between γ-Al_2O_3 and CaO is no longer possible, since they are separated by a layer of the intermediate phase $Ca_{12}Al_{14}O_{33}$. Therefore, the second act of solid-phase interaction in the range of 1000–1100°C will be only between $Ca_{12}Al_{14}O_{33}$ and γ-Al_2O_3 according to reaction (II). Resulted from increasing the calcining temperature to 1200–1250°C the interaction of α-Al_2O_3, localized in the spherulite core, with $CaAl_2O_4$ in the contacting layer according to reaction (III) becomes possible.

$$7\gamma\text{-}Al_2O_3 + 12CaO \rightarrow Ca_{12}Al_{14}O_{33}, \quad \text{(I)}$$

$$Ca_{12}Al_{14}O_{33} + 5\gamma\text{-}Al_2O_3 \rightarrow 12CaAl_2O_4, \quad \text{(II)}$$

$$CaAl_2O_4 + \alpha\text{-}Al_2O_3 \rightarrow CaAl_4O_7. \quad \text{(III)}$$

In the temperature range of 1250–1350°C, all calcium aluminate phases are present (Fig. 5), since reactions (I)–(III) occur simultaneously. The validity of this assumption follows from the results of [14–16], where it was reported that the rate of phase formation in the CaO–Al_2O_3 system is limited by the diffusion of Ca^{2+}, and not by the kinetic factor. For this reason, in the specified temperature range, the concentrations of $CaAl_4O_7$, $Ca_{12}Al_{14}O_{33}$, and $CaAl_2O_4$ are not subject to significant changes, and only a gradual consumption of CaO and α-Al_2O_3 precursors is observed. At temperatures above 1350°C, as noted earlier, the amount of melt in the system increases sharply, which accelerates the counter diffusion of AlO_4^{5-} in the location of CaO concentration. This leads to a significant consumption of α-Al_2O_3 and the synthesis of large quantities of $CaAl_2O_4$ in these zones. As a consequence, calcining of samples of Al-0 composition at 1450°C allows establishing the phase equilibrium and ensuring the design ratio of $CaAl_2O_4$ and $CaAl_4O_7$.

The layered distribution of calcium aluminates, as well as the concentration of α-Al_2O_3 in the center of the grains, are in good agreement with the conclusions of [18, 19]. In the case of samples of Al-2 composition, including pre-ground alumina to D_{50} ~ 10 μm, the phase formation processes proceed in a similar way and in the same sequence as at using unground alumina (D_{50} ~ 90 μm). However, the fundamental difference consists in a decrease in the median size of γ-Al_2O_3 grains from 90 to 10 μm and a significant change in their morphology leads to the formation of calcium aluminates in the temperature range below 1250°C, and also increases the rate of their synthesis. Therefore, it is quite difficult to detect the layered nature of phase formation at small grain sizes. In our opinion, this fact is explained by the synergistic effect of two factors. Firstly, since the processes of synthesis of calcium-aluminate phases in the CaO–Al_2O_3 system are limited by the rate of Ca^{2+} diffusion towards the core of γ-Al_2O_3 grains, a decrease in their size will lead to a reduction in the time of delivery of Ca^{2+} to the reaction zone. An increase in the interfacial surface area also has a positive effect. Secondly, at temperatures up to 1200°C, alumina is in metastable γ- or θ-modifications. Such low-temperature forms of Al_2O_3 are more chemically active than α-Al_2O_3, which, in our opinion, contributes to better diffusion of AlO_4^{5-} groups and an increase in the rate of reactions for the synthesis of calcium aluminates.

At the same time, as follows from the X-ray diffraction analysis data (Figs. 5b, 5f), after calcining at 1250°C, samples of the Al-2 composition do not have the precursors CaO and α-Al_2O_3 and only two phases $CaAl_2O_4$ and $CaAl_4O_7$ are detected in quantities of 85.5 and 13.9 wt %, respectively. Therefore, the question remains open about the mechanism of redistribution of target phases when the calcining temperature increases to 1450°C at the decrease in proportion of $CaAl_2O_4$ to

65.0 wt % and the rise in content of $CaAl_4O_7$ to 35.0 wt %. To clarify the mechanism of such transformation of calcium-aluminate phases in the absence of precursors, additional research is required.

Taking into account the research results reported in this study, a technology for high-alumina cement with an Al_2O_3 content of 71–72 wt % was developed, where by varying the temperature conditions and granulometric composition of the raw ingredients under non-equilibrium conditions, a stable yield of the product with a predominant proportion of the $CaAl_2O_4$ phase is ensured. The novelty of the developed method and the originality of technological methods are confirmed by a patent of the Russian Federation [20]. Currently, the company JSC PKF NK, Stary Oskol, using domestic raw materials (metallurgical alumina of G-00 grade and fine carbonate rock of M-90 grade), has realized industrial production of especially pure high-alumina cement using the technology we developed in a yield of 50 tons per month according to TU (Technical Specification) 23.20.13-081-22298789–2022 "High-alumina cement," which is successfully utilized for the fabrication of low-cement refractory casting mixtures.

CONCLUSIONS

Studies have shown that the use of γ-Al_2O_3, pre-ground to $D_{50} \sim 10$ μm, shifts the processes of formation of the target phases $CaAl_2O_4$ and $CaAl_4O_7$ to the low-temperature region. In our opinion, this is explained by the synergistic effect of two factors: firstly, with a decrease in the size of Al_2O_3 grains, the time of delivery of Ca^{2+} to the reaction zones is reduced; secondly, only metastable forms of Al_2O_3 with very high reactivity participate in the synthesis of calcium aluminate phases. A scheme for the creation of a layered microstructure of calcium-aluminate phases of the core–shell type is proposed. It was shown that by varying the granulometric composition of precursors and heat treatment modes, it is possible to ensure the preferential formation of the $CaAl_2O_4$ phase under nonequilibrium conditions.

ACKNOWLEDGMENTS

The research was carried out using the scientific equipment of the Center for Collective Use "Technologies and Materials" of the National Research University "BelSU".

FUNDING

The work was carried out at the Belgorod State National Research University (NRU "BelSU") with the financial support of the Ministry of Science and Higher Education of the Russian Federation within the framework of agreement dated December 14, 2020, no. 075-11-2020-038 on the implementation of a comprehensive project "Creation of import-substituting production of components matrix systems and thermal engineering composite materials of a new generation based thereon" in accordance with the Decree of the Government of the Russian Federation of 04/09/2010 no. 218.

CONFLICT OF INTEREST

The authors declare that there are no conflicts of interest to disclose in this article.

AUTHOR CONTRIBUTION

M.A. Trubitsyn: selection of research objects, formulation of problems, analysis and processing of the results obtained, analysis of literature data; L.V. Furda: participation in setting problems, analysis of literature data; M.N. Yapryntsev: heat treatment of samples in a high-temperature furnace and studies using X-ray diffraction analysis, participation in the preparation of the section "Results and Discussion," N.A. Volovicheva: carrying out studies of particle size distribution, analysis of the morphology of the surface of materials; M.O. Mikhailyukova: preparation of raw mixtures, analysis of the results of thermal analysis.

REFERENCES

1. *Diagrammy sostoyaniya silikatnykh sistem. Spravochnik. Vypusk pervyi. Dvoinye sistemy* (State Diagrams of Silicate Systems. Directory. First issue. Dual systems), Toropov, N.A., Ed., Leningrad: Nauka, 1969.
2. Rankin, G.A. and Wright, E.F., *Am. J. Sci.,* 1915, vol. s4-39, no. 229, pp. 1–79.
3. Nurse, R.W., Welch J., H., and Majumdar, A.J., *Trans. Brit. Ceram. Soc.,* 1965, no. 64, pp. 409–418.
4. Jerebtsov, D.A. and Mikhailov, G.G., *Ceram. Int.,* 2001, vol. 27, no. 1, pp. 25–28.
   https://doi.org/10.1016/S0272-8842(00)00037-7
5. *Calcium Aluminate Cements: Proceedings of a Symposium Dedicated to H.G.Midgley,* Mangabhai, R.J., Ed., New York: Taylor & Francis, 1990.
   https://doi.org/10.1201/9781482288872
6. Rojas-Hernandez, R.E., Rubio-Marcos, F., Fernandez, J.F., Hussainova, I., *Materials,* 2021, vol. 14,

no. 16, ID 4591.
https://doi.org/10.3390/ma14164591

7. Santos, T., Machado, V.V.S., Borges, O.H., Salvini, V.R., Parr, C., and Pandolfelli, V.C., *Ceram. Int.,* 2021, vol. 47, no. 6, pp. 8398–8407.
https://doi.org/10.1016/j.ceramint.2020.11.204
8. Parreira, R.M., Andrade, T.L., Luz, A.P., Pandolfelli, V.C., and Oliveira, I.R., *Ceram. Int.,* 2016, vol. 42, pp. 11732–11738. https://doi.org/10.1016/j.ceramint.2016.04.092
9. Mohamed, B.M. and Sharp, J.H., *J. Mater. Chem.,* 1997, vol. 7, pp. 1595–1599.
https://doi.org/10.1039/A700201G
10. Rivas Mercury, J.M., De Aza, A.H., and Pena, P., *J. Eur. Ceram. Soc.,* 2005, vol. 25, pp. 3269–3279.
https://doi.org/10.1016/j.jeurceramsoc.2004.06.021
11. Gaki, A., Perrakb Th., and Kakali, G., *J. Eur. Ceram. Soc.,* 2007, vol. 27, no. 2–3, pp. 1785–1789.
https://doi.org/10.1016/j.jeurceramsoc.2006.05.006
12. Rodriguez, M.A., Aguilar, C.L., and Aghayan, M.A., *Ceram. Int.,* 2012, vol. 38, no. 1, pp. 395–399.
https://doi.org/10.1016/j.ceramint.2011.07.020
13. Kurajica, S., Mandic, V., and Sipusic, J., *J. Ceram. Sci. Technol.,* 2011, vol. 2, no. 1, pp. 15–22.
https://doi.org/10.4416/JCST2010-00017
14. Kuznetsova, T.V. and Talaber, I., *Glinozemistyi tsement* (Aluminous Cement), Moscow: Stroiizdat, 1988.
15. Singh, V.K., Ali, M.M., and Mandal, U.K., *J. Am. Ceram. Soc.,* 1990, vol. 73, pp. 872–876.
https://doi.org/10.1111/j.1151-2916.1990.tb05128.x
16. Iftekhar, Sh., Grins, J., Svensson, G., Lööf, J., Jarmar, T., Botton, G.A., Andrei, C.M., and Engqvist, H., *J. Eur. Ceram. Soc.,* 2008, vol. 28, no. 4, pp. 747–756.
https://doi.org/10.1016/j.jeurceramsoc.2007.08.012
17. Trubitsyn, M.A., Yapryntsev, M.N., Furda, L.V., Volovicheva, N.A., Kuzin, V.I., and Zubashchenko, R.V., *Vestn. BGTU im., V.G.Shukhova,* 2022, no. 2, pp. 84–93.
https://doi.org/10.34031/2071-7318-2021-7-2-84-93
18. Trubitsyn, M.A., Furda, L.V., Yapryntsev, M.N., and Volovicheva, N.A., *Russ. J. Inorg. Chem.,* 2022, vol. 67, no. 8, pp. 1308–1318.
https://doi.org/10.1134/S0036023622080277
19. Tian, Y., Pan, X., Yu, H., and Tu, G., *J. Alloys Compd.,* 2016, no. 670, pp. 96–104.
https://doi.org/10.1016/j.jallcom.2016.02.059
20. Patent RU 2794017 (Publ. 2022). *Sposob polucheniya vysokoglinozemistogo tsementa dlya nizkotsementnykh ogneupornykh lit'evykh mass* (Method for Producing High-Alumina Cement for Low-Cement Refractory Casting Masses.).